Ab initio study of the structural properties of acetonitrile–water mixtures

ARTICLE *in* CHEMICAL PHYSICS · JUNE 2015

Impact Factor: 1.65 · DOI: 10.1016/j.chemphys.2015.05.022

2 AUTHORS, INCLUDING:

Jinfan Chen
City University of Hong Kong
3 PUBLICATIONS **23** CITATIONS

Dear Author,

Please, note that changes made to the HTML content will be added to the article before publication, but are not reflected in this PDF.

Note also that this file should not be used for submitting corrections.

Chemical Physics xxx (2015) xxx–xxx

Contents lists available at ScienceDirect

Chemical Physics

journal homepage: www.elsevier.com/locate/chemphys

Ab initio study of the structural properties of acetonitrile–water mixtures

Jinfan Chen, Patrick H.-L. Sit *

School of Energy and Environment, City University of Hong Kong, Kowloon, Hong Kong Special Administrative Region

ARTICLE INFO

Article history:
Received 25 March 2015
In final form 27 May 2015
Available online xxxx

Keywords:
Acetonitrile–water mixtures
Density Functional Theory
Ab initio molecular dynamics
Organic-water solvents
Microheterogeneity

ABSTRACT

Structural properties of acetonitrile and acetonitrile–water mixtures are studied using Density Functional Theory (DFT) and *ab initio* molecular dynamics simulations. Stable molecular clusters consisted of several water and acetonitrile molecules are identified to provide microscopic understanding of the interaction among water and acetonitrile molecules. *Ab initio* molecular dynamics simulations are performed to study the liquid structure at the finite temperature. Three mixing compositions in which the mole fraction of acetonitrile equals 0.109, 0.5 and 0.891 are studied. These compositions correspond to three distinct structural regimes. At the 0.109 and 0.891 mole fraction of acetonitrile, the majority species are mostly connected among themselves and the minority species are either isolated or forming small clusters without disrupting the network of the majority species. At the 0.5 mole fraction of acetonitrile, large water and acetonitrile clusters persist throughout the simulation, exhibiting the microheterogeneous behavior in acetonitrile–water mixtures in the mid-range mixing ratio.

1. Introduction

Acetonitrile (AN) and its mixtures with water are commonly used as reaction media in many different areas like organic synthesis [1,2], reverse phase liquid chromatography [3], electrochemistry [4], phase separation [5], hydrometallurgy [6,7], and atmospheric chemistry [8]. Their popularity arises from the unique characteristics of AN including its large value of dielectric constant and its ability to solvate many inorganic and organic materials [9]. Mixtures of acetonitrile and water provide an additional advantage as their solubility is tunable with different mixing compositions [10].

Due to their widespread applications, many studies have been performed on the structural [9,11–16], thermodynamic [17–21], transport [22,23] and electrical properties [24–26] of acetonitrile–water mixtures. The X-ray diffraction and infrared spectroscopic study on the AN–water mixtures suggested the formation of local clusters of AN in the mixtures. The interactions between AN and water molecules are through both dipole–dipole interaction and hydrogen bonds [9]. From the experimental study of the excess volumes, viscosity, and dielectric constant [19–21], it was debated that the composition of the mixture can be categorized into three structurally distinct regimes. The first regime corresponds to the range of AN mole fraction (x_{AN}) less than around 0.2. In this regime, the AN molecules form isolated clusters in the extended water hydrogen-bond network. The second regime is attained when x_{AN} is between 0.2 and 0.8 where large clusters of water and AN molecules coexist. In this regime, the system is suggested to exhibit spatial inhomogeneities at the microscopic scale but is homogeneous macroscopically [9,12,27]. Such phenomenon is termed microheterogeneity [27–29]. This microheterogeneous characteristic has attracted great interest and debates. Although some studies indicate its existence in the mid-range mixing composition [9,12], other works found no direct evidence for microheterogeneity [13]. The third regime of the mixture corresponds to x_{AN} larger than 0.8, where the water molecules tend to form small clusters or stay isolated which are surrounded by the extended acetonitrile network.

On the other hand, the effect on the water hydrogen-bond network from the addition of dilute AN was also controversial. Infrared spectroscopic studies suggested that the hydrogen-bond network of water is enhanced with the addition of dilute amount of AN [9,13], while other works suggested no such structure enhancement by AN addition [12,30].

Apart from the experimental studies, theoretical works based on classical molecular dynamics methods have been performed on AN–water mixtures. Most of the simulation studies concluded the existence of microheterogeneity in AN–water mixtures by analyzing the radial distribution functions (RDFs) and cluster formation [28,29,31,32]. On the other hand, the effect of dilute AN on the water hydrogen-bond network is more controversial. Kovacs et al. [31] found a slight enhancement of water hydrogen-bond network in the presence of low concentration of AN from the

* Corresponding author. Tel.: +852 34426709.
E-mail address: patrick.h.sit@cityu.edu.hk (P.H.-L. Sit).

http://dx.doi.org/10.1016/j.chemphys.2015.05.022
0301-0104/

analysis of RDFs of water. However, Bakó et al. [32] disagreed and attributed the increased peak heights to the excluded volume effect [33].

Previous theoretical works involved only static *ab initio* studies of isolated AN and water molecular clusters [34–39] or classical molecular dynamics simulations of the liquid mixtures [28,29,31,32]. With more accurate description of the interaction between organic molecules and water and a higher transferability to different mixing conditions, *ab initio* molecular dynamics (MD) provides a powerful tool to reveal the microscopic details of the liquid structure of these mixtures with high accuracy. Such understanding will provide the basis for full-scale *ab initio* studies of various chemical reactions in this class of organic-water solvents. In this work, we first carry out static *ab initio* structural studies of clusters of AN and water molecules. This provides important insights into the microscopic structure of the liquid phase of AN–water mixtures [34–36]. *Ab initio* MD simulations are then performed on AN–water liquid mixtures. To the best of our knowledge, it is the first *ab initio* MD study of AN–water mixtures. Radial distribution functions and cluster formation characteristics are analyzed which reveal the microscopic details of the structural properties of mixtures of AN and water at different mixing compositions.

In Section 2, the computational methods adopted in this work are discussed. We then present the study of the AN and AN–water molecular clusters in Section 3. The *ab initio* MD studies of the AN–water mixtures are also discussed in Section 3. In particular, the radial distribution functions and cluster formation characteristics obtained provide important insight into the microscopic structure of the AN–water mixtures. We summarize the results in Section 4.

2. Computational methods

Density Functional Theory (DFT) studies of the molecular clusters in vacuum were performed using the PWscf module of the Quantum Espresso (QE) package [40] and with the NWChem package [41]. In the calculations using QE, the generalized gradient approximations (GGA) Perdew–Burke–Ernzerhof (PBE) [42] functional, and ultrasoft pseudopotentials [43] were used. Gamma-point sampling was adopted in these calculations with the plane-wave kinetic energy cutoff for the soft-part of the wave-functions and the electronic density chosen as 30 Ry and 240 Ry, respectively. The molecular clusters were situated in vacuum in a cubic unit cell of side length 20 Å, which has been tested to be large enough for the effect of periodic boundary images to be negligible in our systems. In the calculations using NWChem, we used the PBE, B3LYP, PBE0 functionals and the 6-31 + g* basis set. We also carried out simulations with the 6-311++g(2d,2p) basis set. The results are similar to those with 6-31 + g* which suggests that the 6-31 + g* basis set is adequate. Basis set superposition error (BSSE) was corrected by the counter-poise method [44] in the calculations of the interaction energies between molecules.

Car–Parrinello molecular dynamics (CPMD) simulations were carried out with the CP module of QE. The initial configurations for the simulations were obtained from classical molecular dynamics performed with GROMACS [45], and the potential model for water and for AN are SPC/E and OPLS/AA, respectively [46]. The geometries were fully equilibrated within the NVT ensemble for around 10 ns at 300 K. In the CPMD simulations, a fictitious electronic mass of 400 a.u. and a time step of 3 a.u. were employed. The systems were further equilibrated for around 2 ps at 330 K using Car–Parrinello MD, which we have tested to be long enough to obtain the equilibrated structures of the liquid phase. The production runs last for around 5 ps at 330 K after equilibration. Only the PBE functional was used in CPMD simulations. The ultrasoft pseudopotentials and the kinetic energy cutoffs used were the same as those for the molecular cluster calculations with QE. All CPMD simulations are consisted of 64 molecules situated in a cubic unit cell. The densities of the mixtures were chosen to be the experimental values [31]. Three AN–water mixtures compositions with the AN mole fraction of 0.109 (57 water and 7 AN molecules), 0.5 (32 water and 32 AN molecules) and 0.891 (7 water and 57 AN molecules) were studied. These compositions were chosen to correspond to the three distinct regimes of the mixtures [19–21]. The simulations on pure AN and pure water were also carried out for comparison.

3. Results and discussions

3.1. Molecular structures of monomers and clusters of acetonitrile and water

3.1.1. Acetonitrile molecular clusters

Table 1 shows the structural properties and the dipole moment of a single acetonitrile molecule from the PBE, B3LYP and PBE0 functional calculations with the 6-31 + g*, and the PBE functional calculation with the plane-wave basis set. The previous experimental results are also presented in the table for comparison. The atoms in the AN molecules are labeled according to Fig. 1. The geometrical results from different methods agree well with the experimental data. The calculated dipole moments from the localized basis set calculations are also close to the experimental value. However, the dipole moment from the plane-wave calculation with the maximally-localized Wannier function technique is slightly smaller than the experimental value. This discrepancy could be due to the use of periodic boundary conditions and plane-wave basis sets in the calculation.

The structural properties and the interaction energies of dimers, trimers and tetramers of acetonitrile are reported in Tables 2, 3, and 4 respectively. There are multiple values for $R_{N\cdots H}$, $\theta_{N\cdots HC1}$, r_{C2N}, r_{C1C2}, $r_{C1H,}$ θ_{C1C2N}, and θ_{C2C1H} because there are more than one atoms of the same kind in the system. These values are very close and the values shown are the average. The upper case R in $R_{N\cdots H}$ indicates that the atom distance is intermolecular. The corresponding structures are shown in Fig. 2. Overall, the different methods adopted in this work gave similar structural and energetic results.

As shown in Fig. 2, multiple stable structures were obtained for each oligomer size. In particular, we found two stable structures for AN dimers, one in which the two AN molecules align antiparallel to each other (Fig. 2a) and the other in which the two AN molecules align linearly (Fig. 2b). Our calculations with different functionals and basis sets consistently show that the antiparallel configuration is more stable. Despite the structural differences, both structures share the common characteristics that the two molecules interact via the N atom of one AN molecule and the H

Table 1
Comparison of the structural properties and dipole moment of an acetonitrile molecule at different levels of computational method with the 6-31 + g* and plane-wave basis sets. There are three r_{C1H} distances in an AN molecule. The value shown is the average of them. Distances are in Å and angles are in degrees.

	PBE/6-31 + g*	B3LYP/6-31 + g*	PBE0/6-31 + g*	PBE/plane-wave	Experiment [36,47]
r_{C2N}	1.17	1.16	1.16	1.17	1.157
r_{C1C2}	1.46	1.46	1.46	1.46	1.458
r_{C1H}	1.10	1.10	1.09	1.10	1.102
θ_{C1C2N}	180.0	180.0	180.0	179.9	–
θ_{C2C1H}	110.4	110.2	110.2	110.3	109.5
μ (D)	4.03	4.07	4.06	3.42	3.92

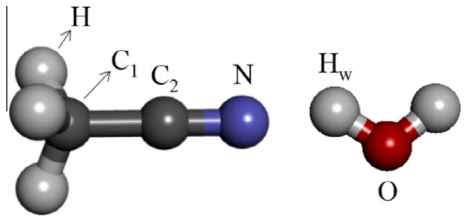

Fig. 1. The atom labels for AN (left) and water (right) molecules. H are the three hydrogen atoms in AN. C_1 is the carbon atom bonded to the H atoms. C_2 is the carbon atom bonded to the N atom. For water, O is the oxygen atom and H_w are the two hydrogen atoms bonded to the oxygen (O) atom.

atoms of the other AN molecule. The antiparallel configuration is more stable because both N atoms are involved in such interaction. Comparing the structural results in Tables 1 and 2, it is found that the intramolecular structure of the AN molecules is little affected by the formation of the dimer, suggesting that the intermolecular interaction is relatively weak, compared to the intramolecular interaction. This is consistent with previous computational [35,36] and experimental [47,48] studies.

Fig. 2c and d show two stable structures for AN trimers. The three ANs either form a ring or align in an antiparallel fashion similar to the dimer in the antiparallel configuration. Table 3 shows the formation energy of the trimers from the molecules. The ring-like geometry is found to be more stable by ~2 kcal/mol. For tetramers, three possible structures were found. The most stable one is a square-like structure with the AN molecules stacking over/below each other (Fig. 2e). The other two possible configurations found have the AN molecules either aligned in an antiparallel conformation (Fig. 2f) or in a square (Fig. 2g). The energy differences between these tetramer structures are small as shown in Table 4, suggesting that the different configurations can readily transform among themselves. This facile transformation can occur more readily as the number of AN increases. Despite the variety of the structural configuration, all the stable structures of dimers, trimers and tetramers display the same characteristics that the N atom of one AN interacts directionally with the H atoms of another.

3.1.2. Acetonitrile–water dimer

Fig. 3a and b show the two optimized structures for AN–water dimers. The structural properties and interaction energies from different calculation methods are listed in Table 5. The atom labels of the water molecule are shown in Fig. 1. In general, different methods gave similar structural results. The two structures obtained are analogous to the linear structure and the antiparallel structure for AN dimers. A hydrogen bond is formed with the N atom in AN acting as the proton acceptor in both cases. Contrary to the case of AN dimers, the linear structure is more stable due to the stronger hydrogen bond formed. This is in agreement with previous simulation works [32,49].

The interaction between two water molecules have been extensively studied [50–53]. We also calculated here the interaction energy between two water molecules using the same set of methods adopted in this work. The values are −6.42 kcal/mol (PBE/6-31 + g*), −6.29 kcal/mol (PBE0/6-31 + g*), −5.79 kcal/mol (B3LYP/6-31 + g*), and −5.30 kcal/mol (PBE/plane-wave). These values are similar in magnitude to the AN–AN (Table 2) and AN–water (Table 5) interaction energies. This explains the high miscibility between AN and water. However, despite the small differences, our calculations show that the water–water interaction is the strongest independent of the method used. The AN–water interaction is slightly weaker and the AN–AN interaction is the weakest. This implies that, in an AN–water mixture, water molecules could preferentially form clusters with other water molecules to maximize the stability.

3.2. Radial distribution functions of AN–water mixtures of different compositions

3.2.1. Acetonitrile–acetonitrile structural correlation

Radial distribution functions from the Car–Parrinello MD simulations are shown in Figs. 4–6. Fig. 4 shows four representative radial distribution functions of atom pairs in AN molecules, namely (a) N—H, (b) N—N, (c) C_1—C_1, and (d) C_2—C_2. The corresponding first peak heights are listed in Table 6. The coordination numbers obtained by integrating the N—H RDFs up to the first minima are also included in the table. The N—H RDF only includes the intermolecular contribution as the intramolecular peak and the first intermolecular peak overlap significantly. This corresponds to the directional interaction between the N atom of one AN molecule and the H atom of another one. The RDFs shown in the Fig. 4 are only for $x_{AN} = 0.5$, $x_{AN} = 0.891$ and pure AN. The ones for $x_{AN} = 0.109$ exhibit large fluctuations due to the small number of AN molecules and the limited simulation time. Therefore, these RDFs are not included in Fig. 4 for comparison but are instead shown in Fig. S1 in the Supporting Information (SI).

The RDFs for different atom pairs for the case of $x_{AN} = 0.5$ and 0.891 (Fig. 4, green lines and blue lines) are qualitatively similar to those of pure AN (Fig. 4, brown lines). This indicates that the AN arrangement is not significantly affected by the addition of water when x_{AN} is 0.5 or higher. However, there is a slight dip in the first peak of the N—H RDF (Fig. 4a) for $x_{AN} = 0.5$ compared to that of the pure AN and $x_{AN} = 0.891$. This peak corresponds to the directional interaction with the N atom of one AN pointing towards the H atom of another AN molecule. This interaction was found in all AN oligomers from our study in vacuum. The slight dip suggests

Table 2
Average intramolecular atomic distances (r_{C2N}, r_{C1C2}, r_{C1H}) and angles (θ_{C1C2N}, θ_{C2C1H}) of AN molecules in the dimers, and the intermolecular distance ($R_{N\cdots H}$) and angle ($\theta_{N\cdots HC1}$) of the directional intermolecular interaction between N and H. In the case of antiparallel configuration (Fig. 2a), the intermolecular molecular distance and angle values shown are the averages of the two directional bonds. In the case of the linearly configuration (Fig. 2b), the intermolecular molecular distance and angle values shown are the averages of the three directional bonds from the same N atom. Interaction energies between molecules of the dimers are also shown. Distances are in Å, angles are in degrees, and interaction energies are in kcal/mol.

	Dimer (Fig. 2a)				Dimer (Fig. 2b)			
	PBE/6-31 + g*	PBE0/6-31 + g*	B3LYP/6-31 + g*	PBE/plane-wave	PBE/6-31 + g*	PBE0/6-31 + g*	B3LYP/6-31 + g*	PBE/plane-wave
$R_{N\cdots H}$	2.59	2.58	2.66	2.56	3.10	3.09	3.15	3.12
$\theta_{N\cdots HC1}$	137.3	136.7	136.6	137.9	91.6	91.3	91.7	91.6
r_{C2N}	1.17	1.16	1.16	1.17	1.17	1.16	1.16	1.17
r_{C1C2}	1.46	1.45	1.46	1.45	1.46	1.46	1.46	1.45
r_{C1H}	1.10	1.09	1.10	1.10	1.10	1.09	1.10	1.10
θ_{C1C2N}	179.0	179.1	179.1	179.1	180.0	180.0	180.0	179.9
θ_{C2C1H}	109.9	109.7	109.8	109.7	110.7	110.4	110.5	110.3
ΔE	−4.72	−4.76	−3.84	−4.67	−2.49	−2.49	−2.11	−2.70

Table 3
Structural properties and the formation energy of acetonitrile trimers from different methods with 6-31 + g* and plane-wave basis sets. $R_{N\cdots H}$ and $\theta_{N\cdots HC1}$ are the average of the intermolecular distances and angles related to the directional interaction between N and H of two of the AN molecules. Distances are in Å, angles are in degrees, energies are in kcal/mol.

	Trimer (Fig. 2c)				Trimer (Fig. 2d)			
	PBE/6-31 + g*	PBE0/6-31 + g*	B3LYP/6-31 + g*	PBE/plane-wave	PBE/6-31 + g*	PBE0/6-31 + g*	B3LYP/6-31 + g*	PBE/plane-wave
$R_{N\cdots H}$	2.32	2.34	2.40	2.30	2.63	2.61	2.70	2.60
$\theta_{N\cdots HC1}$	166.5	164.9	165.3	167.4	136.8	135.8	136.3	137.5
ΔE	−10.55	−10.30	−8.94	−10.60	−8.54	−8.54	−6.93	−8.53

Table 4
Structural properties and the formation energy of acetonitrile tetramers from different methods with 6-31 + g* and plane-wave basis sets. $R_{N\cdots H}$ and $\theta_{N\cdots HC1}$ are the average of the intermolecular distances and angles related to the directional interaction between N and H of two of the AN molecules. Distances are in Å, angles are in degree, energies are in kcal/mol.

	Tetramer (Fig. 2e)				Tetramer (Fig. 2f)				Tetramer (Fig. 2g)			
	PBE/6-31 + g*	PBE0/6-31 + g*	B3LYP/6-31 + g*	PBE/plane-wave	PBE0/6-31 + g*	PBE0/6-31 + g*	B3LYP/6-31 + g*	PBE/plane-wave	PBE/6-31 + g*	PBE0/6-31 + g*	B3LYP/6-31 + g*	PBE/plane-wave
$R_{N\cdots H}$	2.67	2.65	2.74	2.66	2.68	2.67	2.75	2.67	2.31	2.32	2.37	2.29
$\theta_{N\cdots HC1}$	136.5	135.1	135.8	137.0	135.1	133.9	134.7	135.6	179.2	179.0	179.1	179.0
ΔE	−15.24	−15.40	−12.16	−15.28	−15.03	−15.20	−11.96	−15.03	−14.90	−14.65	−12.97	−15.06

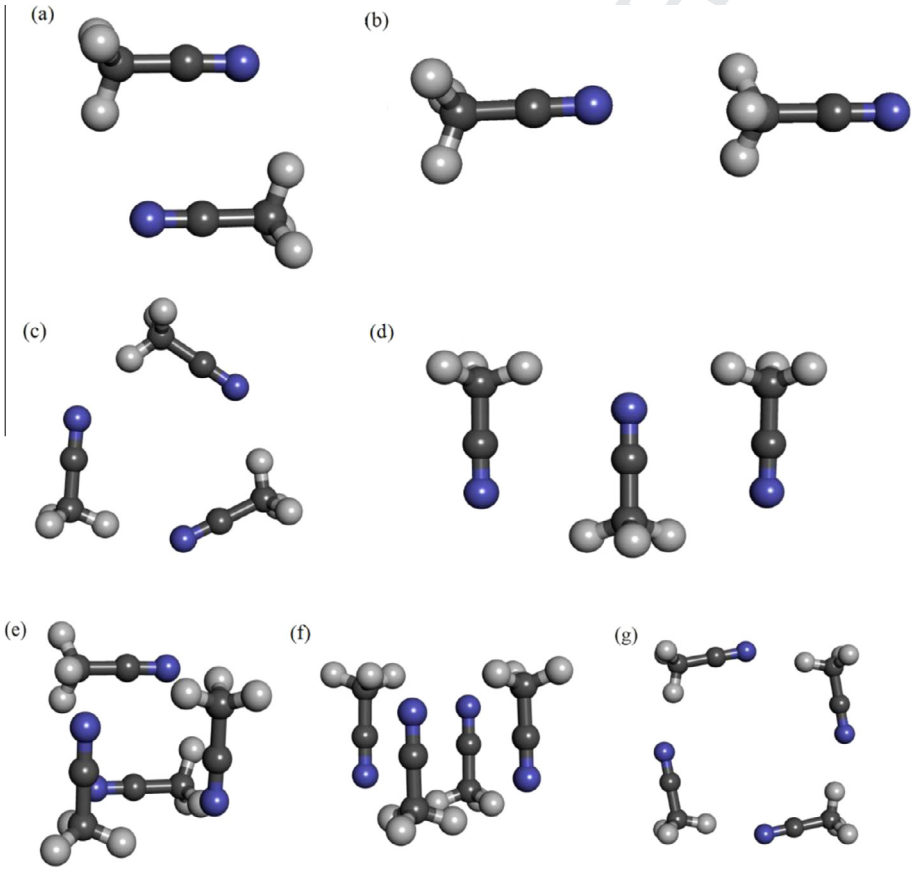

Fig. 2. Optimized structures of acetonitrile dimers, trimers and tetramers.

that the directional interaction has been weakened in the mid-range mixing ratio. However, the N—N RDF (Fig. 4b) for $x_{AN} = 0.5$ is similar to those for $x_{AN} = 0.891$ and pure AN. It indicates that the AN network is not significantly disrupted by water addition although the intermolecular N—H interaction has been weakened. On the other hand, the widths of the first peaks of the C_1—C_1 RDFs (Fig. 4c) and the C_2—C_2 RDFs (Fig. 4d) are wider than those of the N—H RDFs. The larger widths can be explained by the large range of the C_1—C_1 and C_2—C_2 distances found in the molecular arrangements in the AN molecular cluster calculations (Fig. 2) since the local molecular structures in the liquid phase are expected to resemble the structures of the molecular clusters in the vacuum calculations. Lastly, the coordination number for N—H increases when the AN mole fraction increases as shown in Table 6. This suggests that there is an enhancement in AN clustering as the AN mole fraction increases.

Please cite this article in press as: J. Chen, P.-H.L. Sit, Chem. Phys. (2015), http://dx.doi.org/10.1016/j.chemphys.2015.05.022

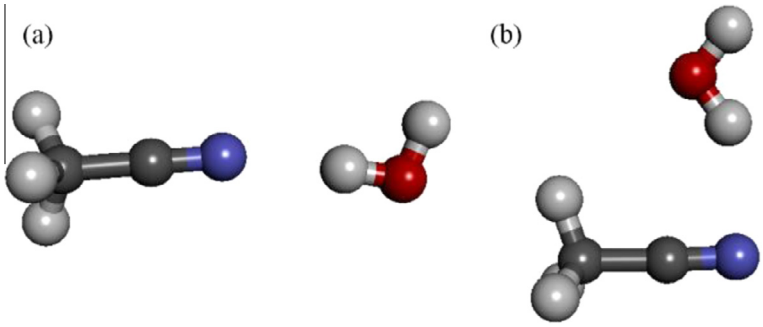

Fig. 3. Optimized structures of an AN–water dimer.

Table 5
Structural properties and the formation energy of acetonitrile–water dimer from different methods with 6-31 + g* and plane-wave basis sets. Distances are in Å, angles are in degree, energies are in kcal/mol.

	Linear (Fig. 3a)				Antiparallel (Fig. 3b)			
	PBE/6-31 + g*	PBE0/6-31 + g*	B3LYP/6-31 + g*	PBE/plane wave	PBE/6-31 + g*	PBE0/6-31 + g*	B3LYP/6-31 + g*	PBE/plane wave
$R_{N\cdots Hw}$	2.05	2.06	2.08	2.02	2.39	2.44	2.43	2.27
$\theta_{\angle OHw\cdots N}$	178.7	177.8	178.4	176.5	139.8	136.8	138.4	146.2
ΔE	−5.02	−4.77	−4.52	−4.92	−4.46	−4.58	−3.95	−3.95

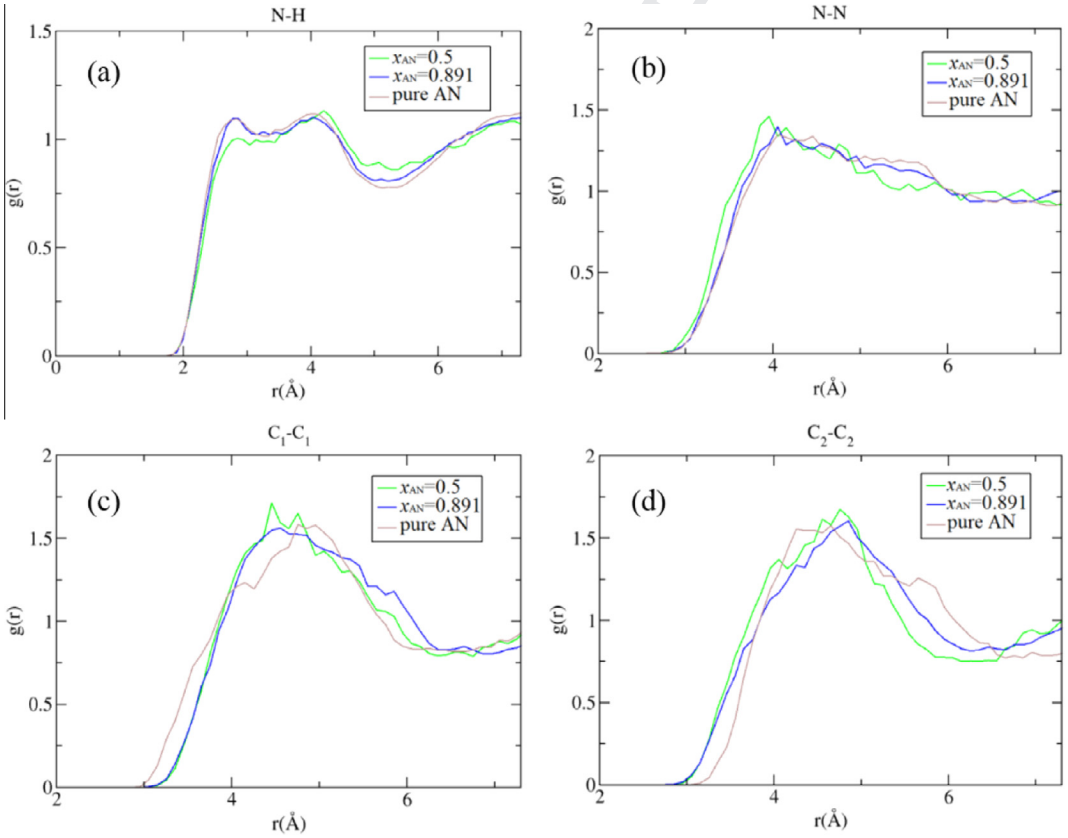

Fig. 4. Radial distribution functions [g(r)] of atom pairs (a) N—H, (b) N—N, (c) C_1—C_1, (d) C_2—C_2 of AN molecules in mixtures with x_{AN} = 0.5 (green), x_{AN} = 0.891 (blue), and pure AN (brown). (For interpretation of the references to color in this figure legend, the reader is referred to the web version of this article.)

3.2.2. Water–water structural correlation

Fig. 5 shows the water–water RDFs between O—O and O—H_w for pure water, and AN–water mixtures with x_{AN} = 0.109 and 0.5. Again, the intramolecular contributions to the O—H_w RDFs are eliminated. The water–water RDFs for x_{AN} = 0.891 exhibit large fluctuations due to limited statistics. They are instead shown in Fig. S2 in the SI. However, the RDFs for water–water at different mixing ratios are in general smoother than those for AN–AN. This is because the smaller size of the water molecules allows faster movement leading to a better sampling of the phase space.

The RDFs for pure water (Fig. 5, black lines) and x_{AN} = 0.109 (Fig. 5, red lines) are similar. However, contrary to the case for

Table 6
The heights of the first peak, g_{peak}, of the radial distribution functions in Fig. 4 and the coordination numbers, n_{coord} obtained by integrating up to the first minima of the N—H RDFs.

x_{AN}	N—H		N—N	C_1—C_1	C_2—C_2
	g_{peak}	n_{coord}	g_{peak}	g_{peak}	g_{peak}
0.5	1.01	3.22	1.46	1.71	1.68
0.891	1.10	4.94	1.40	1.56	1.57
1	1.10	5.26	1.35	1.58	1.58

Table 7
The heights of the first peak, g_{peak}, and the coordination numbers, n_{coord}, integrated up to the first minimum in the radial distribution functions in Fig. 5.

x_{AN}	O—O		O—H_W	
	g_{peak}	n_{coord}	g_{peak}	n_{coord}
0	2.99	4.39	1.59	1.96
0.109	3.33	3.85	1.68	1.71
0.5	5.07	2.33	2.47	1.05

AN–AN correlation, the RDFs at x_{AN} = 0.5 (Fig. 5, green lines) shows significantly larger peaks compared to those for pure water and x_{AN} = 0.109. It was suggested that the increase in peak heights is due to the enhancement of the water hydrogen-bond network in the presence of AN [31]. However, we found that the coordinate number obtained by integrating up to the first minimum decreases as the water-to-AN ratio decreases (Table 7). This is because the integration to obtain the coordination number is weighted by the density of water in the mixtures. Therefore, the increase in the peaks is not due to an enhanced water hydrogen-bond network. This is simply the consequence of the excluded volume effect [33] which leads to the RDFs being significantly above unity in the short-distance region while approaching unity at large distance.

3.2.3. AN–water structural correlation

Fig. 6 shows the RDFs of selected atom pairs of unlike species. The atom pairs are N—O (Fig. 6a), N—H_w (Fig. 6b) and O—H (Fig. 6c). The N—O and N—H_w RDFs show considerably different behaviors at different compositions. In particular, the peak heights become higher and the first minimum becomes deeper as x_{AN} increases. This confirms that these three mixtures compositions, x_{AN} = 0.109, x_{AN} = 0.5 and x_{AN} = 0.891, belong to different structural regimes.

The sharp first peak of the N—H_w RDFs is due to the strong AN–water interaction through hydrogen bonding. As the water composition increases, the peak height decreases because water molecules start to preferentially form hydrogen bonds with other water molecules. The first peaks of the H—O RDFs (Fig. 6c) are not as sharp as those in the N—H_w RDFs (Fig. 6b) because the O atom in water and the H atom in AN are only weakly interacting. The main interaction between AN and water is through N atom in AN and H atom in water, which is consistent with the results from our molecular cluster studies.

Put together, the RDFs pertaining to water–water correlation and AN–water correlation change considerably when the mixture enters the microheterogeneity regime. However, those for AN–AN are less affected. This was also observed in previous classical MD simulations [28]. This was suggested to be due to the fact that the clustering of water, instead of the clustering of AN, is the main driving force of microheterogeneity in the AN–water mixture. Our calculated dimer binding energies and the RDF results support this conclusion.

3.3. Analysis of hydrogen bonding and cluster formation in the acetonitrile–water mixtures

3.3.1. Hydrogen-bond network in the acetonitrile–water mixtures

Previous works on AN–water mixtures [29,32] have focused on the study of the water–water hydrogen-bond network at different mole fractions of AN. Few works have reported on the hydrogen bonds between AN and water or on the AN–AN interactions. Herein, we study the interaction and cluster formation involving AN molecules in AN–water mixtures at different mixing ratios. To define the hydrogen bonds between AN and water, we adopt the same criteria as those used for hydrogen bonds between water molecules [54] – the distance of proton-donating atom (X_1) and proton-receiving atom (X_2) is smaller than 3.5 Å and the X_1–H–X_2 angle is larger than 140°. In the case of AN–water interactions, the X_1 can be either nitrogen or carbon although the directional interaction between the O atom of a water molecule and the H atom of the AN molecule cannot strictly be classified as a hydrogen bond as the proton-donating atom is carbon. For AN–AN interactions, we also adopt in this section the same criteria for "hydrogen bonds" between AN molecules for comparison.

Table 8 shows the number of hydrogen bonds between water and water per water molecule (second row), between AN and water per water molecule (third row), and between AN and AN per AN molecule (fourth row). As x_{AN} increases, the number of water–water hydrogen bonds per water molecule was found to decrease from 3.70 in pure water to 1.28 when x_{AN} = 0.891. The change from pure water to x_{AN} = 0.109 is relatively small, which indicates that the water hydrogen-bond network is not significantly affected by the small mole fraction of AN. The largest change

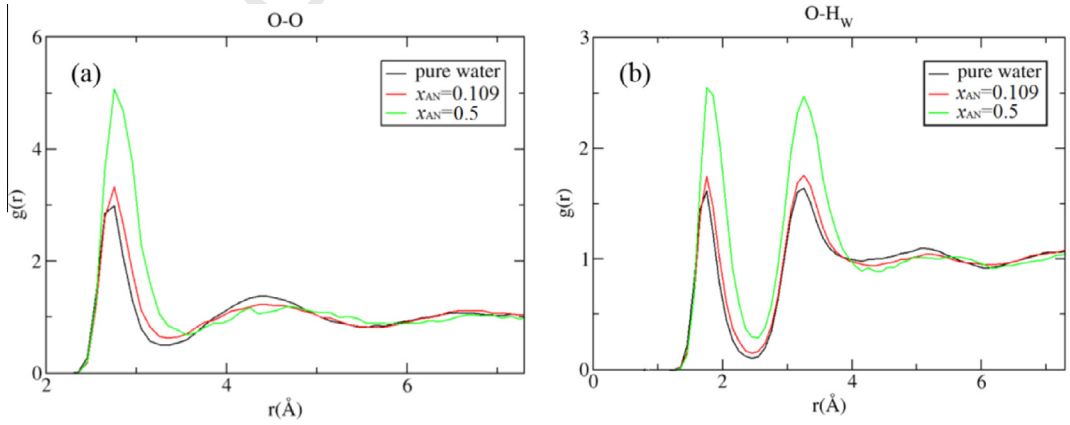

Fig. 5. Radial distribution functions of atom pairs (a) O—O, (b) O—H_W of water in systems of pure water (black), x_{AN} = 0.109 (red), and x_{AN} = 0.5 (green). (For interpretation of the references to color in this figure legend, the reader is referred to the web version of this article.)

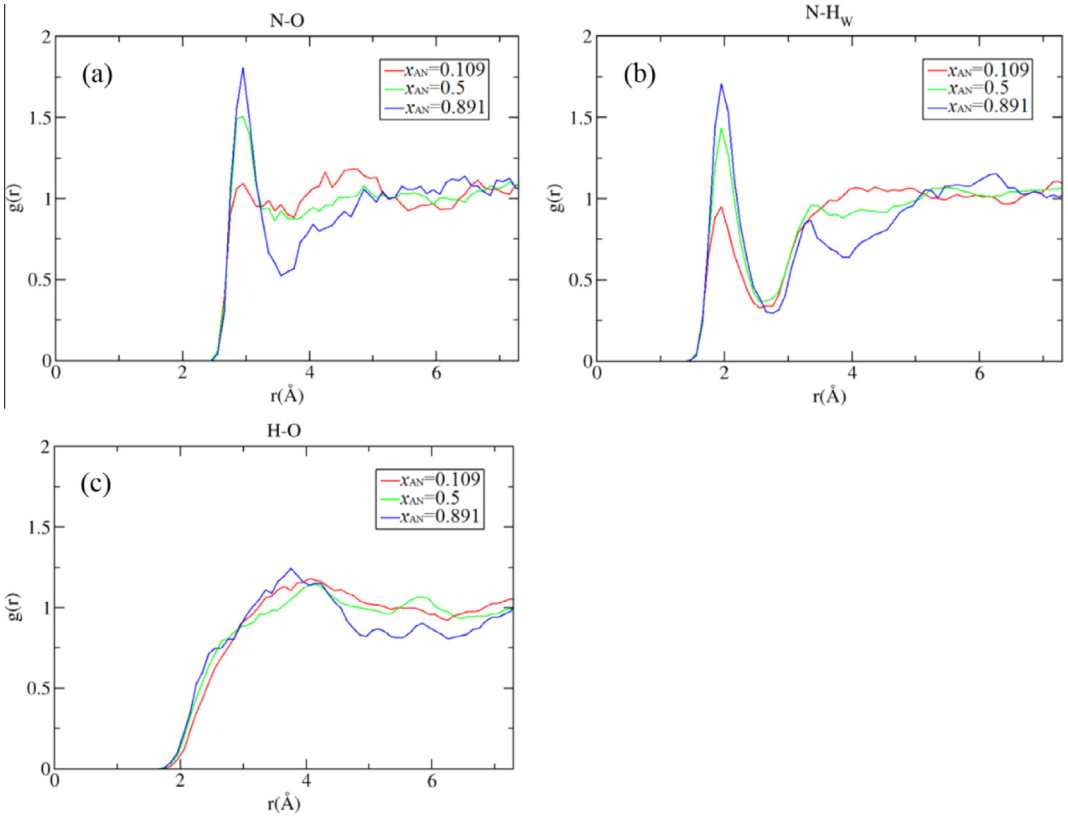

Fig. 6. Radial distribution functions of atom pairs (a) N—O, (b) N—H_W, (c) H—O between AN and water in mixtures of x_{AN} = 0.109 (red), x_{AN} = 0.5 (green) and x_{AN} = 0.891AN (blue). (For interpretation of the references to color in this figure legend, the reader is referred to the web version of this article.)

Table 8
The number of hydrogen bonds between water–water and AN–water per water molecule from the Car–Parrinello molecular dynamics simulations at different mixing compositions (second and third rows). The number of hydrogen bonds per AN molecule from AN–AN molecular dynamics simulations at different mixing compositions (forth row). The values in the parentheses are obtained from the classical molecular dynamics simulations.

System	Pure water	x_{AN} = 0.109	x_{AN} = 0.5	x_{AN} = 0.891	Pure AN
Water–water	3.70(3.49)	3.21(3.19)	1.89(2.23)	1.28(1.03)	–
AN–water	–	0.43(0.35)	1.74(1.40)	2.47(2.56)	–
AN–AN	–	0.06(0.03)	0.46(0.10)	0.67(0.15)	0.75(0.16)

was observed when the AN mole fraction increases from 0.109 to 0.5. In x_{AN} = 0.891, where the water molecules are the minority species, the number of hydrogen bonds per water molecule is still significant, illustrating the persistence of hydrogen bonding interaction at the dilute concentration of water.

The number of AN–water hydrogen bonds per water molecules increases from 0.43 when x_{AN} = 0.109 to 2.47 when x_{AN} = 0.891. When x_{AN} = 0.5, the value is 1.74, which is comparable to 1.89, the number of water–water hydrogen bonds at the same x_{AN}. This shows that hydrogen bond plays an important role in connecting AN and water molecules. This finding is in contrast to a previous experimental work which suggested that AN and water interact mostly through dipole–dipole interactions [55].

The number of "hydrogen bonds" formed by pairs of AN molecules per AN molecule grows with increasing x_{AN}, from 0.06 when x_{AN} = 0.109 to 0.75 in pure AN. The number of hydrogen bonds changes more significantly from x_{AN} = 0.109 to x_{AN} = 0.5, and varies to a lesser extent from x_{AN} = 0.5 to pure AN. This suggests that the largest change in the AN structure occurs in the small x_{AN} regime while the change from pure AN to x_{AN} = 0.5 is relatively small.

Classical molecular dynamics simulations with the GROMACS package [45] were also used to study AN–water mixtures at different compositions. The simulation unit cell in the classical MD also contains 64 molecules. The simulations were equilibrated for 1 ns and the production runs last for 10 ns at 300 K. The numbers of hydrogen bonds per molecule from the classical MD simulations are listed in the parentheses in Table 8. As shown in the table, there is a general agreement in the number of hydrogen bonds formed by water–water and AN–water per water molecule between *ab initio* MD and classical MD (second and third row, Table 8). However, the classical MD simulations consistently underestimate the number of "hydrogen bond" between two AN molecules (forth row, Table 8). Especially in the AN-rich systems, x_{AN} = 0.891 and pure AN, the numbers of hydrogen bonds per AN molecule are only 0.15 and 0.16, respectively, which are much smaller than those from the *ab initio* MD (0.67 for x_{AN} = 0.891 and 0.75 for pure AN). The directional interaction between the N atom of an AN and the H atom of the other AN is more accurately described by the *ab initio* technique.

Previous Raman and NMR experimental works [23,56] studied the mole fraction of AN which are hydrogen-bonded to water in the mixtures. They found that at low AN concentration, the majority of AN are hydrogen-bonded to water through the N atom. These AN are termed 'bound' AN. The number of bound AN increases as the AN mole fraction increases until x_{AN} is around 0.5. Beyond that, AN molecules that are not hydrogen-bonded through the N atom to water ('free' AN) become dominant. We calculated from our simulations the mole fraction of 'bound' and 'free' AN at the three mixing ratios (Table 9). These values agree very well with the experimental results [23].

Table 9
The mole fraction of 'bound' and 'free' AN in AN–water mixtures at each mixing ratio.

System	x_{AN} = 0.109	x_{AN} = 0.5	x_{AN} = 0.891
x_{bound}	0.094	0.28	0.091
x_{free}	0.015	0.22	0.80

3.3.2. Water cluster size analysis in the acetonitrile–water mixtures

Analysis of the cluster size formed by the AN or water molecules provides key information of the structural characteristics in the AN–water mixtures. In this subsection, we focus on the formation of water clusters. A water molecule is considered to be part of a water cluster if it is connected to other water molecules in the cluster through hydrogen bonding. Several key parameters were chosen, listed below, to describe the cluster formation characteristics. The analysis is along the same line as the previous works performed with classical MD [32,57].

N: the total number of water molecules;
$\boldsymbol{N_u}$: the average number of unbonded water molecules that are not involved in forming clusters with other water molecules;
$\langle \boldsymbol{n} \rangle$: the average water cluster size, defined by the number of water molecules within the cluster ($\langle n \rangle = \sum_{n\geqslant 1} n m_n / \sum_{n\geqslant 1} m_n$, n is the cluster size, m_n is the number of the clusters with size n);

Table 10
The total number of water molecules, the average number of unbonded water molecules and the average water cluster size in AN–water systems at different mixing ratios.

System	Pure water	x_{AN} = 0.109	x_{AN} = 0.5	x_{AN} = 0.891
N	64	57	32	7
N_u	0.01	0.15	2.75	1.02
$\langle n \rangle$	64	49	7	3

Table 10 shows these parameters for water clusters at different mixing compositions. For comparison, the data from the pure liquid water simulation are also provided. We also estimated the expected errors for $\langle n \rangle$ from the 5-ps CPMD simulations using long classical MD simulations. The estimation procedure is discussed in details in the SI. The errors are of the order of unity. Therefore, $\langle n \rangle$ shown in Table 10 are rounded to the nearest unit digit. As shown in the table, the average cluster size is 64 and the value of N_u is only 0.01 for pure water. The water molecules tend to form one extended cluster with all water molecules essentially connected to each other. In the AN–water mixture with x_{AN} = 0.109, the average cluster size is reduced to 49 compared to the total number of water molecules of 57 in the mixture. The average number of unbonded molecules is 0.15. Most of the water molecules still tend to form one large cluster, similar to that of the pure water. This suggests that the extended water network stays intact. When the mole fraction of AN is increased to 0.5, the average cluster size drops to 7. The extended water structure starts to break and the system evolves into a different structural regime. In the x_{AN} = 0.891 mixture, the water molecules form small clusters or stay isolated within AN structure network. Among the 7 water molecules in x_{AN} = 0.891, there are on average 1.02 isolated molecules and the average water cluster size is 3. Clusters involving several water molecules persist in the mixture with a high mole fraction of AN.

Fig. 7 shows the average number of water molecules involved in water clusters of different sizes at different mixing compositions. For pure water, almost all water molecules are involved in forming one extended cluster. In the x_{AN} = 0.109 mixture, the majority of water molecules form one large cluster similar to the pure water case but with a higher proportion of isolated water molecules. When x_{AN} = 0.5, water clusters with different sizes are formed. Water molecules in x_{AN} = 0.891 tend to form small clusters involving several molecules. The cluster size distribution results show

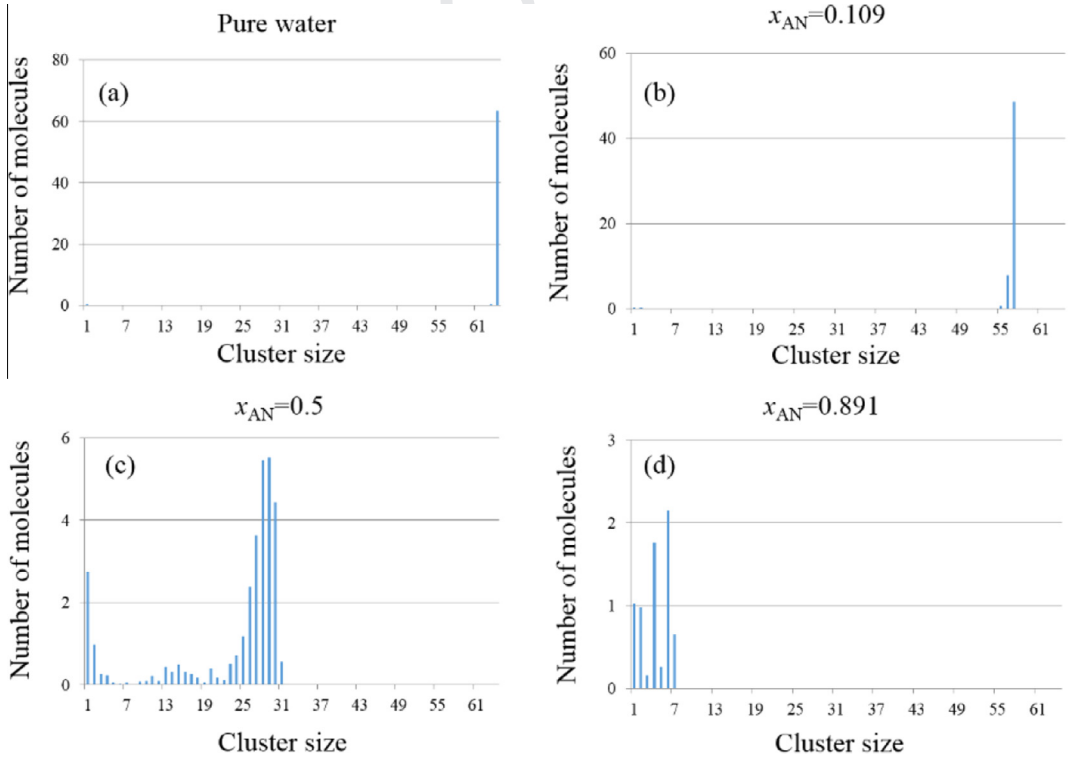

Fig. 7. Size distribution of water clusters connected through hydrogen bond in (a) pure water, (b) x_{AN} = 0.109, (c) x_{AN} = 0.5, (d) x_{AN} = 0.891. The y-axis is the average number of water molecules involved in water clusters of a certain size. The x-axis is the size of the water cluster.

Please cite this article in press as: J. Chen, P.-H.L. Sit, Chem. Phys. (2015), http://dx.doi.org/10.1016/j.chemphys.2015.05.022

that the x_{AN} = 0.109, 0.5 and 0.891 mixtures exhibit very different characteristics in the water structure which indicates that these mixtures are in different structural regimes.

3.3.3. Acetonitrile cluster size analysis in the acetonitrile–water mixtures

The small number of "hydrogen bonds" formed between AN–AN as shown in Table 8 compared to that of water–water or AN–water indicates that hydrogen bonding is not the governing interaction between AN molecules. To better describe cluster formation of AN molecules, we adopt here a less stringent criterion in which only the atomic distance is considered. As discussed earlier, the AN molecules tend to connect to each other with the N atom pointing towards the H atom of other AN. We therefore pick the length of the first minimum in N—H RDF, d_{N-H} = 3.5 Å, as the cutoff distance. The parameters used to analyze AN cluster formation are defined below which are similar to those for water in Section 3.3.2.

N: the total number of AN molecules;
$\boldsymbol{N_u}$: the average number of unbonded AN molecules that are not involved in forming clusters with other AN molecules;

$\langle \boldsymbol{n} \rangle$: the average AN cluster size, defined by the number of AN molecules within the cluster.

Table 11
The total number of AN molecules, the average number of unbonded AN molecules and the average AN cluster size in AN–water systems at different mixing ratios. When the N atom of one AN and the H atom of another AN is closer than 3.5 Å criterion, the two AN molecules are considered connected.

System	x_{AN} = 0.109	x_{AN} = 0.5	x_{AN} = 0.891	Pure AN
N	7	32	57	64
N_u	2.12	0.00	0.00	0.00
$\langle n \rangle$	2	32	57	64

Table 11 shows these parameters in the AN–water mixtures and pure AN. The AN cluster size distributions are displayed in Fig. 8. $\langle n \rangle$ shown are also rounded to the nearest unit digit. For x_{AN} = 0.109, we found that the 7 AN molecules in the mixture prefer to form small clusters with the average size of 2 molecules per cluster. Combining with the water–water cluster formation discussed in Section 3.3.2, it can be concluded that the small AN clusters are situated within the extended water hydrogen-bond network without disrupting the extended water structure. For x_{AN} = 0.5, the average AN cluster size is 32 molecules which is very close to the total number of AN of 32 in the mixture. For x_{AN} = 0.891 and pure AN, all AN molecules in the mixtures form one extended cluster throughout the simulation time. The cluster characteristics of x_{AN} = 0.5 and x_{AN} = 0.891 closely resemble that of pure AN, which suggests that the AN network keeps intact from pure AN to x_{AN} = 0.5. Combining with the results in Section 3.3.2, when x_{AN} = 0.891, the small water clusters are likely to situated within the extended AN network without causing any disruption. On the other hand, when x_{AN} = 0.109, AN molecules form small clusters within the extended water network. Lastly, the x_{AN} = 0.5 mixture is in a special regime which large clusters of water and AN are separately formed exhibiting the microheterogeneous characteristics. This agrees well with the experimental studies [9,16,55,58,59]. One should note that the unit cell side length of the x_{AN} = 0.5 simulation was 15.452 Å. Such microscopic density inhomogeneity of length-scale of several Angstroms [9,16,28] is within the size of our simulation.

Fig. 9 shows the snapshots with the structural characteristics in different mixing regimes. At x_{AN} = 0.109 and 0.891 (Fig. 9a and c), the majority species form an extended cluster and the small clusters of the minority species are situated within the extended network. At x_{AN} = 0.5 (Fig. 9b), large clusters of water and AN are formed separately. In this particular snapshot, the water molecules are connected together around the upper half of the cubic

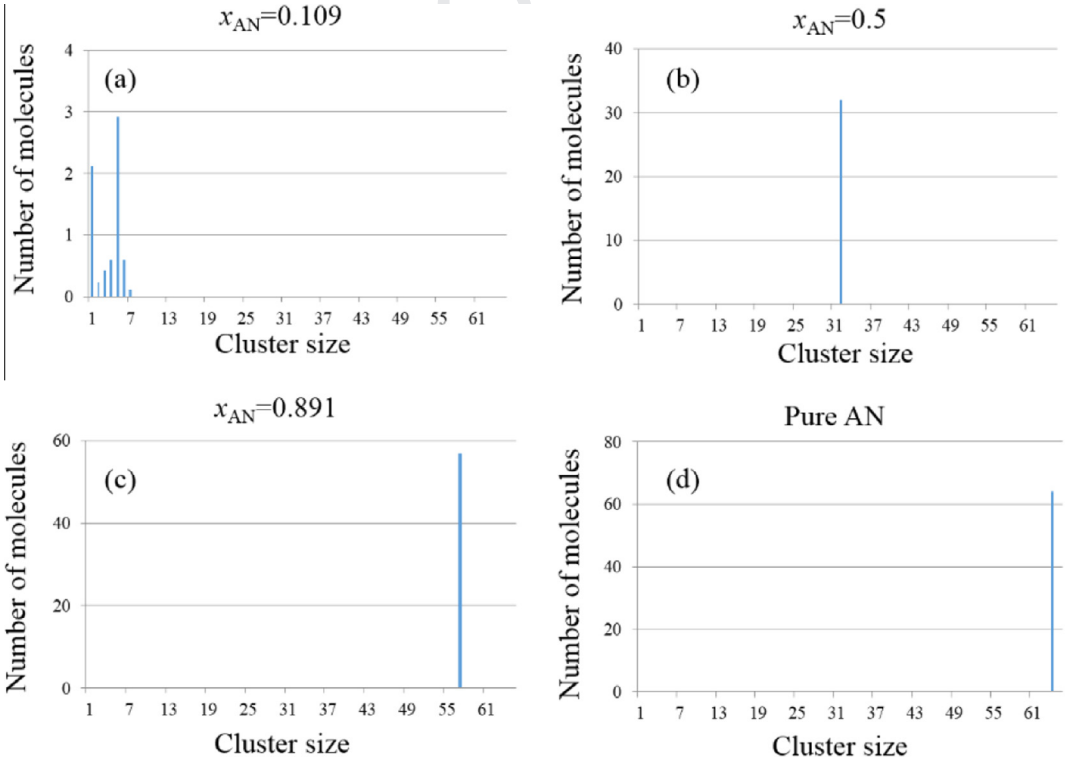

Fig. 8. Number and size distribution of AN clusters defined through critical N—H atom distance in (a) x_{AN} = 0.109, (b) x_{AN} = 0.5, (c) x_{AN} = 0.891, (d) pure AN. The *y*-axis is the average number of AN molecules involved in AN clusters of a certain size. The *x*-axis is the size of the AN cluster.

Please cite this article in press as: J. Chen, P.-H.L. Sit, Chem. Phys. (2015), http://dx.doi.org/10.1016/j.chemphys.2015.05.022

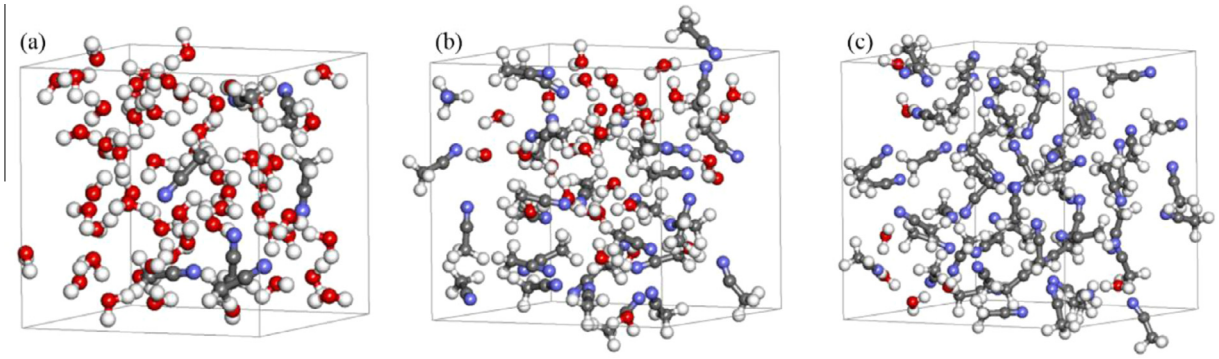

Fig. 9. Snapshots from the simulations of the AN–water mixtures with the mole fraction of AN equals (a) 0.109, (b) 0.5, and (c) 0.891, respectively.

simulation box and the AN molecules are mainly in the lower half, exhibiting the distinct microheterogeneous behavior.

4. Summaries and conclusions

DFT calculations and *ab initio* molecular dynamics simulations were carried out to study the structural properties of molecular clusters and of the liquid mixtures of AN and water. The study of AN molecular oligomers in vacuum shows the "hydrogen-bond-like" directional interaction with the N atom of one AN molecule pointing towards one of the H atoms of another AN molecule. On the other hand, AN and water molecules were found to interact similarly by hydrogen bonding with the AN molecule acting solely as the proton acceptor.

The structural properties of AN–water mixtures with different mixing ratios were studied in detail with *ab initio* MD. In pure AN, in the $x_{AN} = 0.891$ mixture and in the $x_{AN} = 0.5$ mixture, the RDFs related to AN–AN structural correlation were found to be similar. Analysis of the cluster size in these liquids showed that the AN molecules are mostly connected together to form one large cluster. In the $x_{AN} = 0.109$ mixture, the AN molecules form small clusters and are situated within the extended water network. On the other hand, the RDFs related to water–water structural correlation for pure water and for the $x_{AN} = 0.109$ mixture are similar. However, from $x_{AN} = 0.109$ to $x_{AN} = 0.5$, the RDFs change significantly. Analysis of the water cluster size also shows similar water cluster formation characteristics in pure water and in the $x_{AN} = 0.109$ mixture. But there are significant differences when x_{AN} is increased from 0.109 to 0.5. Further changes were found when x_{AN} was raised to 0.891. Combining the structural information of AN and water clusters, $x_{AN} = 0.109$, $x_{AN} = 0.5$ and $x_{AN} = 0.891$ can be concluded to correspond to three distinct regimes characterized by different local structures of AN and water. In particular, when $x_{AN} = 0.5$, we observed the microheterogeneous behavior in which extended water and AN clusters coexist. In the case for $x_{AN} = 0.109$ and $x_{AN} = 0.891$, the minority species are either isolated or forming small clusters situated within the network of the majority species.

The different structural regimes in AN–water mixtures were also identified from the study of the number of hydrogen bonds per molecule. Using geometrical criteria for bond length and bond angle to define a hydrogen bond, the numbers of water–water hydrogen bonds and AN–water hydrogen bonds per water molecule were found to change significantly as x_{AN} changes from 0.109 to 0.5, and from 0.5 to 0.891. For AN–AN interaction, we adopted the same criteria although this is not strictly a hydrogen bond. The numbers of "hydrogen bond" formed by AN–AN in the $x_{AN} = 0.5$ mixture, the $x_{AN} = 0.891$ mixture and pure AN were found to be similar which is much larger than that in the $x_{AN} = 0.109$ mixture.

Previous studies [9,13,31] suggested that the addition of dilute AN enhances the network of the water molecules. In this work, we found that, while the first peak height of the RDFs related to water–water structural correlation increases as x_{AN} increases, the number of first solvation shell water molecules of a water molecule decreases. Therefore, no enhancement was observed upon addition of dilute AN.

Acetonitrile–water mixtures are ubiquitous as the reaction media in numerous areas due to their unique properties. In this work, we reveal the microscopic structural characteristics of these solutions at different mixing compositions using extensive DFT and *ab initio* MD simulations. Future work could involve the inclusion of van der Waals corrections to investigate the effect of weak interactions on the liquid structure. For liquid water, previous studies have shown that the structure and dynamics can be affected by the van der Waals corrections [60–63]. In particular, the density is increased while the liquid structure is softened and the diffusivity is enhanced with the corrections. In conclusion, the understanding of the structural properties at the atomistic scale is crucial for full-scale *ab initio* studies of different chemical reactions in acetonitrile–water solutions, which provide important insights into the design of better chemical processes.

Acknowledgments

The authors acknowledge the support by the CityU Start-up Grant (Project No. 7200397) and the CityU SRG Fund (Project No. 7004166).

Appendix A. Supplementary data

Supplementary data associated with this article can be found, in the online version, at http://dx.doi.org/10.1016/j.chemphys.2015.05.022.

References

[1] M. Reslow, P. Adlercreutz, B. Mattiasson, Eur. J. Biochem. 177 (1988) 313.
[2] G. Sabitha, R.S. Babu, M. Rajkumar, J.S. Yadav, Org. Lett. 4 (2002) 343.
[3] J. Braun, A. Fouqueau, R.J. Bemish, M. Meuwly, Phys. Chem. Chem. Phys. 10 (2008) 4765.
[4] Y. Tomita, S. Teruya, O. Koga, Y. Hori, J. Electrochem. Soc. 147 (2000) 4164.
[5] P.B. Dhamole, P. Mahajan, H. Feng, J.S. Chem. Eng. Data 55 (2010) 3803.
[6] A.J. Parker, D.M. Muir, D.E. Giles, R. Alexander, J. O'Kane, J. Avraamides, Hydrometallurgy 1 (1975) 169.
[7] P. Singh, B.W. Clare, C.C. Kenna, D.M. Muir, Electrochim. Acta 31 (1986) 535.
[8] C.A. Deakyne, M. Meot-Ner, C.L. Campbell, M.G. Hughes, S.P. Murphy, J. Chem. Phys. 84 (1986) 4958.
[9] T. Takamuku, M. Tabata, A. Yamaguchi, J. Nishimoto, M. Kumamoto, H. Wakita, T. Yamaguchi, J. Phys. Chem. B 102 (1998) 8880.

[10] Y. Marcus, J. Phys. Org. Chem. 25 (2012) 1072.
[11] K.L. Rowlen, J.M. Harris, Anal. Chem. 63 (1991) 964.
[12] D. Jamroz, J. Stangret, J. Lindgren, J. Am. Chem. Soc. 115 (1993) 6165.
[13] D.S. Venables, C.A. Schmuttenmaer, J. Chem. Phys. 108 (1998) 4935.
[14] I. Bakó, T. Megyes, T. Grósz, G. Pálinkás, J. Dore, J. Mol. Liq. 125 (2006) 174.
[15] T. Takamuku, Y. Noguchi, M. Nakano, M. Matsugami, H. Iwase, T. Otomo, J. Ceram. Soc. Jpn. 115 (2007) 861.
[16] T. Takamuku, Y. Noguchi, M. Matsugami, H. Iwase, T. Otomo, M. Nagao, J. Mol. Liq. 136 (2007) 147.
[17] J. Catalán, C. Díaz, F. García-Blanco, Org. Biomol. Chem. 1 (2003) 575.
[18] R.H. Stokes, J. Chem. Thermodyn. 19 (1987) 977.
[19] C. Moreau, G. Douhéret, J. Chem. Thermodyn. 8 (1976) 403.
[20] C. Moreau, G. Douhéret, Thermochim. Acta 13 (1975) 385.
[21] G. Douhéret, C. Moreau, A. Viallard, Fluid Phase Equilib. 22 (1985) 289.
[22] K.R. Harris, P.J. Newitt, J. Phys. Chem. B 103 (1999) 7015.
[23] E.D. Dawson, S.L. Wallen, J. Am. Chem. Soc. 124 (2002) 14210.
[24] L.G. Gagliardi, C.B. Castells, C. Rafols, M. Rosés, E. Bosch, J. Chem. Eng. Data 52 (2007) 1103.
[25] R. Jellema, J. Bulthuis, G. Van der Zwan, J. Mol. Liq. 73 (1997) 179.
[26] M.I. Davis, G. Douhéret, Thermochim. Acta 104 (1986) 203.
[27] Y. Marcus, Y. Migron, J. Phys. Chem. 95 (1991) 400.
[28] R.D. Mountain, J. Phys. Chem. B 114 (2010) 16460.
[29] D.L. Bergman, A. Laaksonen, Phys. Rev. E 58 (1998) 4706.
[30] J.E. Bertie, Z. Lan, J. Phys. Chem. B 101 (1997) 4111.
[31] H. Kovacs, A. Laaksonen, J. Am. Chem. Soc. 113 (1991) 5596.
[32] I. Bakó, T. Megyes, G. Pálinkás, Chem. Phys. 316 (2005) 235.
[33] A.K. Soper, J. Phys.: Condens. Matter 9 (1997) 2399.
[34] S. Nigam, C. Majumder, J. Chem. Phys. 128 (2008) 214307.
[35] E.M. Cabaleiro-Lago, J.M. Hermida-Ramón, A. Pena-Gallego, E. Martınez-Núnez, A. Fernández-Ramos, J. Mol. Struct.: THEOCHEM 498 (2000) 21–28.
[36] R.A. Mata, B.J. Costa, THEOCHEM 673 (2004) 155.
[37] M. Albertí, A. Amat, F. De Angelis, F. Pirani, J. Phys. Chem. B 117 (2013) 7065.
[38] G. Del Mistro, A.J. Stace, J. Chem. Phys. 99 (1993) 4656.
[39] B. Mennucci, C.O. da Silva, J. Phys. Chem. B 112 (2008) 6803.
[40] P. Giannozzi, S. Baroni, N. Bonini, M. Calandra, R. Car, C. Cavazzoni, D. Ceresoli, G.L. Chiarotti, M. Cococcioni, I. Dabo, J. Phys.: Condens. Matter 21 (2009) 395502.
[41] M. Valiev, E.J. Bylaska, N. Govind, K. Kowalski, T.P. Straatsma, H.J.J. Van Dam, D. Wang, J. Nieplocha, E. Apra, T.L. Windus, W.A. de Jong, Comput. Phys. Commun. 181 (2010) 1477.
[42] J.P. Perdew, K. Burke, M. Ernzerhof, Phys. Rev. Lett. 77 (1996) 3865.
[43] D. Vanderbilt, Phys. Rev. B 41 (1990) 7892.
[44] S.F. Boys, F. Bernardi, Mol. Phys. 19 (1970) 553.
[45] E. Lindahl, B. Hess, D. Van Der Spoel, J. Mol. Model. 7 (2001) 306.
[46] W.L. Jorgensen, J. Tirado-Rives, Proc. Natl. Acad. Sci. USA 102 (2005) 6665.
[47] C.C. Costain, J. Chem. Phys. 29 (1958) 864.
[48] H. Bertagnolli, P. Chieux, M.D. Zeidler, Mol. Phys. 32 (1976) 759.
[49] A. Chaudhari, S.L. Lee, Int. J. Q. Chem. 102 (2005) 106.
[50] E. Schwegler, J.C. Grossman, F. Gygi, G. Galli, J. Chem. Phys. 121 (2004) 5400.
[51] T.R. Dyke, K.M. Mack, J.S. Muenter, J. Chem. Phys. 66 (1977) 498.
[52] L. Curtiss, D. Frurip, M. Blander, J. Chem. Phys. 71 (1979) 2703.
[53] P.-H.-L. Sit, N. Marzari, J. Chem. Phys. 122 (2005) 204510.
[54] J.C. Grossman, E. Schwegler, G. Galli, J. Phys. Chem. B 108 (2004) 15865.
[55] N. Huang, D. Nordlund, C. Huang, U. Bergmann, T.M. Weiss, L.G. Pettersson, A. Nilsson, J. Chem. Phys. 135 (2011) 164509.
[56] J.R. Reimers, L.E. Hall, J. Am. Chem. Soc. 121 (1999) 3730.
[57] A. Geiger, F. Stillinger, A. Rahman, J. Chem. Phys. 70 (1979) 4185.
[58] T. Takamuku, A. Yamaguchi, D. Matsuo, M. Tabata, M. Kumamoto, J. Nishimoto, K. Yoshida, T. Yamaguchi, M. Nagao, T. Otomo, T. Adachi, J. Phys. Chem. B 105 (2001) 6236.
[59] K. Nishikawa, Y. Kasahara, T. Ichioka, J. Phys. Chem. B 106 (2002) 693.
[60] J. Wang, G. Román-Pérez, J.M. Soler, E. Artacho, M.V. Fernández-Serra, J. Chem. Phys. 134 (2011) 024516.
[61] R. Jonchiere, A.P. Seitsonen, G. Ferlat, A.M. Saitta, R. Vuilleumier, J. Chem. Phys. 135 (2011) 154503.
[62] A. Tkatchenko, R.A. DiStasio Jr., R. Car, M. Scheffler, Phys. Rev. Lett. 108 (2012) 236402.
[63] R.A. DiStasio Jr., B. Santra, Z. Li, X. Wu, R. Car, J. Chem. Phys. 141 (2014) 084502.